Journal of Applied Polymer Science

Development and Oxygen Scavenging Performance of Three-Layer Active PET Films for Food Packaging

Luciano Di Maio, Paola Scarfato, Maria Rosaria Galdi, Loredana Incarnato
Department of Industrial Engineering, University of Salerno, Via Giovanni Paolo II, 132 - 84084, Fisciano (Salerno), Italy
Correspondence to: P. Scarfato (E-mail: pscarfato@unisa.it)

ABSTRACT: Polymeric active materials represent an innovative food packaging concept that has been introduced to improve the quality of foods and to enhance their shelf life. In this article, the effect of the inclusion of an oxygen scavenger in a polymeric matrix, realizing multilayer active polyester films by coextrusion process, is analyzed. In particular, three layer active films, at different mass ratios of the layers, were produced to form symmetrical "ABA" structures comprising polyethylene terephthalate (PET) with a polymeric oxygen scavenger (OS) as core layer and pure PET as external layers. Oxygen scavenging tests conducted on the multilayer active structures have pointed out the role of the relative layer thickness in controlling the scavenging capacity, the activity time and the oxygen absorption rate. A modeling of the scavenging phenomena, which combines a quasi steady-state distribution in the skin layers with a flat profile of O_2 content in the active core layer, can explain the experimentally observed oxygen absorption rate at short times. Moreover, steady state oxygen transport measurements, performed when the scavenger reactive capacity is exhausted, have shown that the presence of the active phase slightly reduces the O_2 permeability, compared with the neat PET. The effect, which progressively increases with the amount of active phase in the film formulation, was related to the different morphological state developed on processing. Finally, preliminary shelf life tests on fresh-cut untreated apples suggest that the developed three layer active films have a significant potential in the shelf-life extension of oxygen sensitive food products. © 2014 Wiley Periodicals, Inc. J. Appl. Polym. Sci. **2015**, *132*, 41465.

KEYWORDS: films; manufacturing; packaging; polyesters; properties and characterization

Received 8 April 2014; accepted 27 August 2014
DOI: 10.1002/app.41465

INTRODUCTION

In recent years, there is a growing interest in the design of innovative and ecological polymeric barrier packaging systems to prolong the shelf life of many oxygen-sensitive foods and beverages.[1]

Currently, solutions for increasing barrier properties consist of high-barrier multilayer laminates, polymeric blends, or coated films by silica, aluminium, and polymeric resins.[2–5] All these systems are defined as passive barriers, since they strongly reduce the gases flow through the side wall by preserving the package headspace composition over time. However, this class of materials, even coupled with modified atmospheres (MAP), not always represents the best solution to prolong the shelf life of fresh and oxygen sensitive foods.[6,7] Moreover, for many products the consumers prefer films, which are transparent and yet still flexible.

A recent strategy for making better barrier films involves the incorporation of active molecules into polymeric matrix to realize active packaging. This technology can modify the internal composition of the packaging according to food's needs and retards penetration of solutes like oxygen as they diffuse across the film. Thus, the active packages could allow to preserve the sensory characteristics of products, ensuring their freshness.[8–17] Among the active systems applied to food packaging, the oxygen scavengers (OS) are widely studied as the food deterioration is mainly governed by oxidation processes.[18–24] The most common OS technology consists in permeable sachets that contain the oxygen absorbent components and that are normally included in the package. However, the sachets cannot be used for liquid products and the consumers are still wary about these solutions because the sachets are visible and they could be source of food contamination. Therefore, the addition of oxygen scavengers to polymeric matrices during the extrusion process represents a very promising approach for producing active packages for several kinds of food.

In the case of polyester-based active packaging, the oxygen scavengers investigated are wide and complex, as described by the academic and patent literature.[25–36] These active scavengers are generally modified copolyamides activated by cobalt salt, active copolyesters obtained by grafting polyester chains with unsaturated polyolefin oligomers, micrometals and nanometals, and active nanocomposites.

Table I. Relative Mass Ratios and Thickness of Material Forming Each Layer of Coextruded Films

Sample	External layers/ active core layer relative mass ratios	External/active core/external layer thicknesses (microns)
SL-PET	100/0	17.5/0/17.5
TL1	70/30	13.0/9.0/13.0
TL2	60/40	10.75/13.5/10.75
TL3	50/50	9.0/17.0/9.0
SL-APET	0/100	0/35.0/0

The overall film thickness is 35 microns.

The active integrated packaging applications are mostly relative to bottles and trays, given the complexity in achieving active transparent thin films by mean of traditional production processes.

In our previous works, monolayer active polyethylene terephthalate (PET) films at different concentrations of an oxygen scavenger (from 1 wt % to 20 wt %) were produced in laboratory and analyzed in order to investigate the effect of composition on the structure and the properties of the active films.[37,38] The results highlighted that the monolayer active film at 10 wt % weight of the selected OS (Amosorb DFC 4020) was the most performing among the compositions analyzed. Moreover, the activity of monolayer films saturates in few days because of the fast reaction with oxygen of the active phase.[38]

With the aim to further increase the reaction time of these active PET-based films, a symmetrical three-layer structure of "ABA" type was designed to protect the internal active polyester layer from fast oxidation, by means of two external layers of pure PET. The use of one resin (monomaterial) makes the structure completely recyclable at "end of life," too, with positive effect on its environment friendliness.

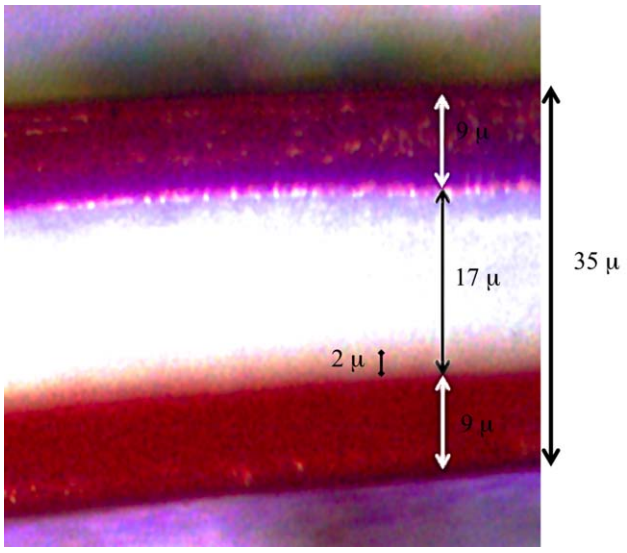

Figure 1. Optical microscopy image of the active three-layer film TL3 (section normal to the extrusion direction), coextruded using a red colored pigment added to the external neat PET layers (magnification 100×). [Color figure can be viewed in the online issue, which is available at wileyonlinelibrary.com.]

To verify the effectiveness of such solution in prolonging the films activity, the produced samples were submitted to oxygen absorption analyses in continuous mode. These measurements have let to determine the scavenging properties of the active films, and specifically the initial oxygen scavenging rate, the scavenging capacity and the activity time. The kinetic of the scavenging phenomena at short times resulted in good agreement with the behavior predicted by a model that combines a quasi steady-state distribution in the skin layers with a flat profile of the oxygen content in the active core layer.

Finally, the active film capability in preserving the quality of oxygen sensitive foods was preliminarily assessed by performing packaging experiments, using fresh cut apple slices as model food, and comparing the effect of the different used films on the changes in color, acidity, and sugar content of the apples over time.

EXPERIMENTAL

Materials

The selected matrix is the film grade PET resin Cleartuf P60 (M&G Polimeri S.p.A., Patrica (FR), Italy), having intrinsic viscosity 0.58 dL/g. The active scavenger is Amosorb DFC 4020 (AMS, supplied by Colormatrix Europe, Liverpool, UK). It is a copolyester-based polymer designed for rigid PET containers, characterized by an auto-activated scavenging mechanism.[27,33] Both PET and AMS comply fully with FDA and EU food contact legislation.

Red masterbatch (RENOL®-ne/C, supplied by Clariant) was used in preliminary coextrusion process experiments in order to calibrate and optimize the relative layer thickness and distribution.

Processing

Conditioning. The PET was dried under vacuum at 130°C for 16 h, before processing. The AMS, delivered dried in aluminum bags sealed under vacuum, was used as received.

Film Production. The films were manufactured by making use of a laboratory coextrusion cast film line (Collin, Teach-line E20T), equipped with three single screw extruders ($D = 20$, $L/D = 25$), a flow convergence system (feed-block), a coat-hanger type head (slit die of 200 × 0.25 mm^2) and a take-up/cooling system (chill rolls) thermally controlled by water circulation at 10°C. The die temperature was set at 285°C, whereas the temperature profile along the extruder was constant at 280°C, for all the extruders. The chill roll speed was 7 m/min, thus allowing films stretching to their final dimensions (about 170 mm wide and 35 μm thick).

Symmetrical structures of three layers from two materials of "ABA" type, where the external layers are made of neat PET and the core layer is made of active PET (i.e., PET loaded with 10 wt % of AMS), were produced with different mass flow rate ratios of the layers, maintaining a constant total extruded mass

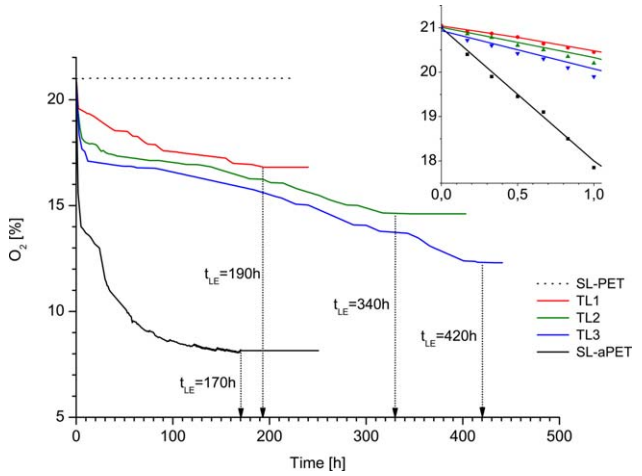

Figure 2. Oxygen absorption kinetics at 23°C for the single layer neat (SL-PET) and active (SL-aPET) PET films and for the three layer (TL1, TL2, and TL3) film samples, with different relative layer thickness. Inset graph: zoom of the region at short times [the individual points represent the experimental data, whereas the lines represent the data calculated according to eqs. (4), (13), and (14)]. [Color figure can be viewed in the online issue, which is available at wileyonlinelibrary.com.]

rate of 5.85 kg/h. The AMS concentration in the core layer was chosen on the basis of previous published results.[38]

Single layer films made of neat PET and active PET (i.e., PET loaded with 10 wt % of AMS) were also produced, for comparison, using the same apparatus and processing conditions.

The nomenclature and the composition of all produced film samples are reported in Table I.

Before producing films for testing, a preliminary study on the layer distribution during the coextrusion process was performed. At this regard, the external layers of neat PET were colored with 0.1 wt % of red master-batch, so that the three layers were well distinguishable in the films. Therefore, their relative thicknesses were measured by optical microscope analyses and related to their relative mass flow ratios.

Characterization Methods

Optical microscopy (OM) observations were performed by means of a Zeiss Axioskop microscope (Carl Zeiss Vision, Germany) on film sections cut normally to the extrusion direction by cryofracture of the film in liquid nitrogen.

The oxygen absorption measurements were carried out at 23°C in continuous mode by means of the fiber optical oxygen meter Minisensor Oxygen Fibox 3-Trace V3 (PreSens GmbH, Regensburg, Germany), equipped with sensor coating type PSt3 (detection limit 15 ppb, 0–100% oxygen). The tests were performed on samples with a defined geometry (5 × 5 cm^2 and about 35 μm thick), sealed in the measurement cell having volume equal to 70 mL.

Table II. Scavenging Capacity (μ) and Exhaustion Time (t_{LE}) for SL-aPET, TL1, Tl2, and TL3 Active Films, at 23°C

Sample	μ $\left[\frac{mg\,O_2}{g\,film}\right]$	μ $\left[\frac{mg\,O_2}{g\,AMS}\right]$	t_{LE} (h)
TL1	1.10	42.8	190
TL2	1.70	44.1	340
TL3	2.13	43.8	420
SL-aPET	4.68	46.8	170

The oxygen permeability of the produced films was assessed by means of a gas permeabilimeter (GDP-C, Brugger, Munchen Germany). The tests were carried out in triple at 23°C and 75% R.H., with the oxygen flow rate of 80 mL/min (ISO 15105-1). In order to reach the equilibrium value of permeability, the films were also analyzed after the complete scavenger saturation. The standard deviation of the permeability coefficient results are in the worst case contained within 1.5% of the reported value.

The thermal behavior of the films was analyzed by mean of a differential scanning calorimeter (DSC) (mod. DSC 822, Mettler Toledo) on samples as extruded. The specimens were heated at a rate of 10°C/min from 25°C to 300°C under a nitrogen gas purge (50 mL/min), in order to minimize thermo-oxidative degradation phenomena. Crystallinity degrees, X_c, of the different films were determined according to the following equation:

$$X_c = \frac{\Delta H_m - \Delta H_C}{(1-\phi)\cdot \Delta H_m^0} \quad (1)$$

where ΔH_m and ΔH_{cc} are the heat of melting and the heat of cold crystallization of the film sample, respectively, ΔH_m^0 is the heat of melting of the purely crystalline PET, that is, 117 J/g and ϕ is the AMS weight percentage in the sample.[39]

The effect of the three layer active films in preserving the quality of fresh fruits was preliminarily verified analyzing the browning over time of untreated fresh-cut apple slices (Golden Delicious cultivar) packaged with them. At this purpose, packages (13 × 13 cm^2) were produced by thermo sealing the active and PET films at 120°C for 1 s and applying a sealing force of 500N by mean of a thermosealing lab machine (HSG-C–Heat-Sealing Machine-Brugger Feinmechanik GmbH). Five packages for each film sample were realized in order to evaluate the effect of active films compared with pure PET on apple preservation. These packages were filled with two slices (~40 g) of untreated Golden Delicious apples, completely sealed and then stored in a refrigerator at 8°C. The quality of the apple slices during the storage was determined measuring their color variation and evaluating their acidity and sugars content over time.

The color of fresh-cut apple slices was measured on homogeneous spot areas of 4 mm in diameter, by means of a colorimeter Minolta CR-300 (Konica Minolta International, Japan). The color difference of the same apple slice over time, reported as $\Delta E_{CMC(1:1)}$, was determined according to the method of the Colour Measurement Committee (Society of Dyes and Colourists of Great Britain) CMC(1 : 1) based on the CIELAB color difference components ΔL^*, ΔC^*ab, and ΔH^*ab.[40] It includes two parameters: lightness weighting (l) and chroma weighting (c), allowing the users to weight the difference based on the ratio of l : c. The 1 : 1 ratio is recommended for "perceptibility" decisions. $\Delta E_{CMC(1:1)} \approx 1$ corresponds to a just noticeable difference.[41]

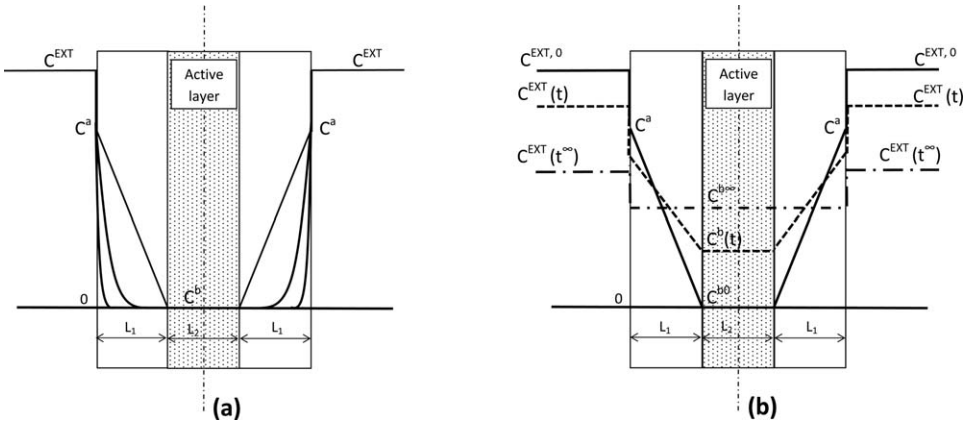

Figure 3. Qualitative development of concentration profiles during (a) the initial transient state "stage I" ($t = 0$) and (b) the pseudo steady state condition stage II in the three layers active PET film. C^{EXT} represents the O_2 concentration in the test vial, C^a is the equilibrium concentration at the external interface and C^b represents the O_2 concentration in the active layer (C^{b1}, C^{b2}, and $C^b\infty$ are the O_2 concentration in the active layer at times t^1, t^2, and t^∞ respectively).

The total acidity was determined by dilution of 20 g of crushed apple samples into 100 mL distilled water and potentiometric titration with 0.1 *N* NaOH up to pH 8.1.

The sugars content was determined by HPLC (Agilent 1100 Series), using a system equipped with a controller and a differential refractometer. The column used was Hypersil NH2 (150 × 4.6 mm i.d. column); the mobile phase was acetonitrile/water 80/20 v/v; the flow rate was 1 mL/min. Before the analyses, the apple slices were ground in 50 mL deionized water and then they were centrifuged for 15 min, transferred into a volumetric flask and diluted to 100 mL with water. Finally, 25 mL of clarified extract were filtered through a 0.45-μm membrane and analyzed.

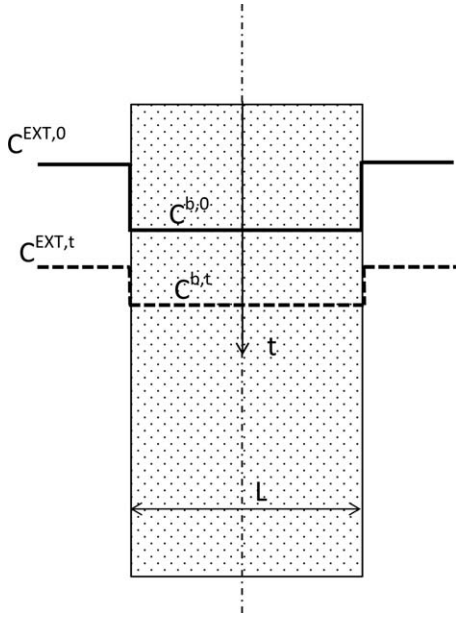

Figure 4. Qualitative development of concentration profiles in the single layer active PET film of thickness L. C^{EXT} represents the O_2 concentration in the test vial and C^b represents the O_2 concentration in the active layer.

RESULTS AND DISCUSSION

The three-layer coextruded films were preliminarily investigated by OM in order to verify the uniformity of the layer's shape and thickness, which play a key role in the development of the overall film properties. The OM analysis was performed on all the symmetric structures produced according to the processing conditions specified in the Experimental section, using a red-colored pigment (0.1 wt %) added to the external neat PET layers, so to make clear the location of the interface (a series of experiments were conducted that showed no significant influence of the addition of low levels of pigment on the flow properties of the resin). Figure 1 reports the image taken on TL3 structure, chosen as an example. The OM observations clearly show that, under the working conditions used in our study, all the co-extruded films have layers with flat interfaces and constant thickness along the transversal film section. Moreover, two interdiffusional regions about 2-μm thick at layer interfaces can be observed, too. The relative layer thicknesses measured by OM on all the produced films, and reported in Table I, are fairly in accordance with the corresponding external/core mass ratios used during the co-extrusion. The small deviations can be related to the change in the viscoelastic response of the PET resin because of AMS addition.[38]

In order to evaluate the oxygen scavenging properties of the three-layer active films, absorption analyses in continuous mode were performed. The obtained oxygen absorption kinetics are reported in Figure 2, together with those of the single layer neat and active PET films, for comparison. The graph shows that the neat PET film does not have any reactivity, as expected, whereas all the active films immediately react with the oxygen inside the cell, absorbing it over time and reaching a plateau value after a specific time interval depending on the system composition, pointing out the end of the sample's activity.

The analysis of the oxygen absorption curves has allowed calculating the main absorption properties of all the active films, such as the initial oxygen scavenging rate (i.e., the slope of each curve at short times), the exhaustion time t_{LE} (i.e., the time within the tested sample loses completely its activity and the

Table III. Values of Parameters and Constants Used for Calculating the Data from eqs. (4), (13), and (14)

Description	Parameters	Values	Units
Oxygen diffusivity	D	4.81×10^{-9}	cm^2/s
Volume of head space	V^{HS}	70	mL
Initial concentration of scavenger	$C^{SC,0}$	0.01186	mol/L
Initial concentration of O_2 at $t = 0$	$C^{EXT,0}$	8.561×10^{-3}	mol/L
Solubility coefficient	S	7.16×10^{-2}	$cm^3/(cm^3 \cdot bar)$
Area	A	25	cm^2
Kinetic constant	k	1.0×10^4	$cm^3/mol\ s$
Stoichiometric factor	K	1	-

oxygen concentration assumes a constant value) and the scavenging capacity μ the ratio between the volume of oxygen absorbed by the films during the test and their weight). All the obtained results are reported in Table II.

The oxygen scavenging in polymeric films is a complex, heterogeneous process, involving the coexistence of physical and chemical phenomena such as the physical dissolution and diffusion of the gas through the polymer and reaction of the active phase with oxygen.[42] Many efforts are present in the literature devoted to model these phenomena in order to predict the performance of scavenging films pointing out that there is a strong difference between the behavior of multilayers and single layer systems.[43–46].

In general, the analysis of multilayers films can be performed as a case of one-dimensional diffusion in a medium bounded by parallel planes sheets of material so thin that effectively all the diffusing substance enters through the plane faces and a negligible amount through the edges. In particular, for the system under scrutiny it is reasonable to consider an initial transient period, followed by a pseudo steady-state phase (Figure 3). According to Figure 3(a), where the concentration profiles of the oxygen within film are qualitatively reported, during the first stage a transient diffusion occurs until a linear concentration gradient of the oxygen through the external layer of the polymer is developed. The scavenging activity of the active layer is considered constant and the oxygen concentration C^b is zero at the interface between the nonactive and the active layer because of a reaction speed much higher than the diffusion (i.e., the process is controlled by diffusion). In the second step [Figure 3(b)], the linear concentration gradient will evolve due to the decreasing scavenging effect in the active layer related to the consumption of the active component. The oxygen concentration in the active layer in this case is considered uniform through the thickness with values that gradually increase with time (from C^{b0} to $C^{b\infty}$, which is the concentration within the central layer at sorption equilibrium with the external gas phase).

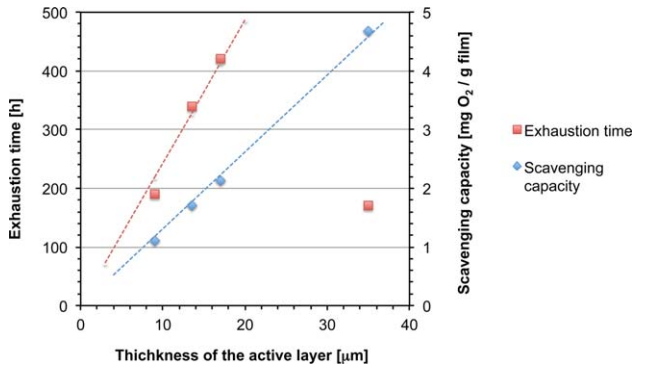

Figure 5. Dependence of both exhaustion time (t_{LE}) and scavenging capacity (μ) on the thickness of the active layer of the films, for the single layer active PET (SL-aPET) and the three layer (TL1, TL2, and TL3) systems. [Color figure can be viewed in the online issue, which is available at wileyonlinelibrary.com.]

Under the aforementioned assumptions it is possible to calculate the O_2 concentration $C^{EXT}(t)$ in the test vial as a function of time:

$$C^{EXT}(t) \cdot V^{\text{head space}} = C^{EXT,0} \cdot V^{\text{head space}} - Q(t) \cdot A \qquad (2)$$

where $Q(t)$ is the total amount per unit area (mol/m^2) of oxygen diffused through the two external surfaces of PET film at time t and $C^{EXT,0}$ represents the initial concentration of O_2 at time 0. In view of the simplifying hypothesis that two different stages–in the following '*stage I*' and '*stage II*'–of diffusion/reaction process can be identified, we illustrate here how the corresponding values of $Q(t)$, respectively $Q^I(t)$ and $Q^{II}(t)$, can be evaluated.

$Q^I(t)$, which is the $Q(t)$ evaluated during the initial transient stage during the time t^I, can be calculated as follows:[47]

$$Q^I(t) = 2 \cdot L_1 C^a \left[\frac{Dt}{L_1^2} - \frac{1}{6} - \frac{2}{\pi^2} \sum_{n=1}^{\infty} \frac{(-1)^n}{n^2} \cdot \exp\left(-\frac{Dn^2\pi^2 t}{L_1^2} \right) \right] \qquad (3)$$

where C^a is the O_2 concentration (retained as constant during the stage I) at the film surface, D is the O_2 diffusivity through the nonactive PET layer and L_1 is its thickness. It is here assumed that, during the first stage, the consumption of scavenger is negligible, the most part of its decrease occurring in the second stage. Equation 3 describes the oxygen sorption process till the establishment of a linear profile of oxygen concentration within the external layer, that is, till time t^I.

Table IV. Oxygen Transport Coefficients Evaluated at 23°C After Scavenger Saturation

Sample	O_2TR [cm^3/(m^2·d·bar)]	$D_{O2} \times 10^9$ [cm^2/s]	$S_{O2} \times 10^2$ [cm^3/(cm^3·bar)]	$P \times 10^{10}$ [cm^3·cm/(cm^2 s·bar)]	
				Experimental	Calculated according to eq. (15)
SL-PET	84.9	4.81	7.16	3.44	-
TL1	86.2	4.80	7.27	3.49	3.02
TL2	76.0	4.52	6.81	3.08	2.85
TL3	59.5	3.80	6.33	2.41	2.71
SL-aPET	55.3	2.43	9.20	2.24	-

The corresponding mass balance expression for the concentration of the scavenger within the inner core is the following, in the time interval $0 < t < t^I$:

$$C^{Sc,\ I}(t) \cdot L_2 \cdot A = C^{Sc,0} \cdot L_2 \cdot A - K \cdot Q^I(t) \tag{4}$$

where K is a stoichiometric factor for the reaction occurring between oxygen and scavenger. In analyzing the second stage of the process (i.e., from time t^I to ∞), which sets up at longer times, it is assumed that pseudo steady conditions hold. As a consequence, $Q^{II}(t)$ has the following expression:

$$Q^{II}(t) = \int_{t^I}^{t} \left(2A \cdot D \cdot \frac{C^a(t) - C^b(t)}{L_1} \right) dt \tag{5}$$

where the generic t is greater than t^I. Both C^a and C^b are changing with time. The mass balance for the scavenger moiety is as follows, in the time interval from t^I to ∞:

$$C^{Sc,\ II}(t) = C^{Sc,I}(t^I) - \int_{t^I}^{t} kC^b(t) \cdot C^{Sc,\ II}(t) dt \tag{6}$$

where k is a kinetic constant and it has been assumed that the elementary step for reaction involves 1 oxygen and 1 scavenger mole. The evolution of C^a can be calculated from the corresponding value of C^{EXT} from sorption thermodynamics, that is:

$$C^a(t) = S \cdot C^{EXT}(t) \tag{7}$$

Eqs. (2), (5), (6), and (7) represent the system to be solved to determine the evolution of O_2 concentration within the head space volume of the vial during the second stage of the process.

In summary, the concentration of oxygen in the vial headspace in the full time interval can be evaluated from eq. (2) using:

$$Q(t) = Q^I(t) \text{ for } 0 < t < t^I \tag{8}$$

and

$$Q(t) = Q^I(t^I) + Q^{II}(t) \qquad \text{for } t^I < t < \infty. \tag{9}$$

The experimental results reported in Figure 4 are consistent with the above analytical approach and the O_2 consumption appears related to the nonactive layer thickness.

As far as the behavior of the single layer active film is concerned, also in this case the development of concentration profiles will follow a nonsteady state process characterized by a variation of the O_2 flow rate through the film that will depend on time due to the decreasing of both the scavenging effect and the O_2 concentration within the head space. However, if the analysis is focused only at the early stages of the process, it is possible to consider a reaction controlled process (i.e., diffusion is much faster than reaction) and the concentration of O_2 in the film (C^b) as uniform. Thus, the following mass balance for O_2 in the vial will apply:

$$V^{\text{HEAD SPACE}} \cdot \frac{dC^{EXT}}{dt} = -kC^b(t) \cdot C^{sc}(t) \cdot L \cdot A \tag{10}$$

where L and A are the film thickness and the total exposed area of the sample, respectively.

The mass balance on the oxygen scavenger can be written as:

$$\frac{dC^{sc}}{dt} = -kC^b(t) \cdot C^{sc}(t) \cdot L \cdot A \tag{11}$$

By keeping the previous hypotheses the following relationship between the O_2 concentration in the polymer (C^b) and in the vial (C^{EXT}) apply:

Table V. Thermal Parameters of film Samples

Sample	T_g (°C)	T_m (°C)	T_c (°C)	ΔH_m (J/g)	ΔH_c (J/g)	X_c (%)
SL-PET	74	254	133	46.1	32.8	11.4
TL1	76	252	135	52.0	36.1	13.9
TL2	76	250	133	53.1	38.5	13.0
TL3	78	252	136	52.3	38.3	12.6
SL-aPET	74	250	125	44.7	44.7	15.6

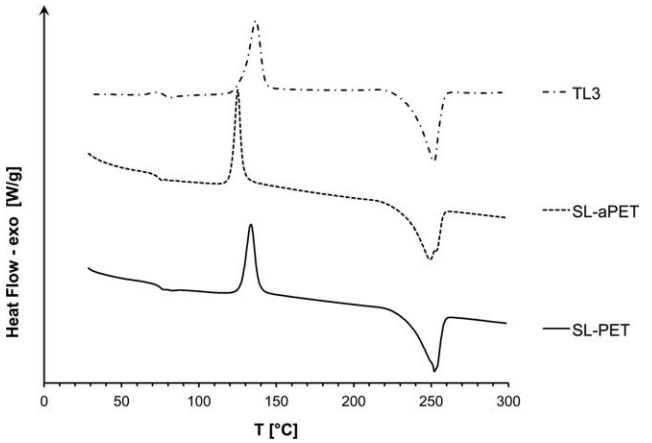

Figure 6. Comparison among the DSC thermograms of the single layer neat (SL-PET) and active (SL-aPET) PET films and the three layer (TL3) film samples.

$$C^{b}(t) = S \cdot C^{EXT}(t) \tag{12}$$

The substitution of eq. (12) in eqs. (10) and (11) yields the following system:

$$\frac{dC^{EXT}}{dt} = -\frac{kLA}{V^{HEAD\ SPACE}} \cdot S \cdot C^{EXT}(t) \cdot C^{sc}(t) \qquad C^{EXT} = C^{EXT,0} \text{ at } t = 0 \tag{13}$$

$$\frac{dC^{sc}}{dt} = -k \cdot S \cdot C^{EXT}(t) \cdot C^{sc}(t)\, C^{SC} = C^{SC,0} \qquad \text{at } t = 0 \tag{14}$$

It is worth noting that, according to the experimental results, the values of oxygen concentration, calculated at short times from the equations (4), (13), and (14) using the parameters and the constants of Table III, present a faster decrease for the single layer active film respect to the multilayer films, as shown in Figure 2.

Among all tested active films, the SL-aPET one shows the highest initial oxygen scavenging rate, as expectable considering that in this system the active phase is homogeneously distributed in the whole film and then it is directly exposed to the air. In comparison, the three-layer films have an oxygen scavenging rate always lower and progressively decreasing with the increase of the thickness of the external neat PET layers (from TL3 to TL1), as the oxygen has to diffuse through these layers before it can react with the active phase contained in the core of the film.

Correspondingly, also the exhaustion times are always longer than that of the SL-aPET system (~170 h) and progressively increase with the thickness of the external neat PET layers, passing from ~190 h for the TL3 film to 420 h for the TL1 one. This occurs despite the active layer in the three-layer structures is thinner than in the SL-aPET one, namely despite in the three-layer structures there is a lower amount of AMS available for the oxidation. On the contrary, the scavenging capacity μ, evaluated for each sample as the volume of oxygen absorbed by the film weight at its exhaustion time, increases with the increase of the internal PET active layer thickness. However, the scavenging capacity μ, evaluated for each sample as the volume of oxygen absorbed by the active layer weight at its exhaustion time is not significantly different among all the active systems, suggesting that the structure and properties of the active layers are almost identical independently from the film structure and composition.

With the aim to better clarify the correlation between activity and composition of the tested active three-layer and single layer films, Figure 5 shows the dependence of both the exhaustion times and the scavenging capacity μ on the thickness of the active layer of the films. The graph clearly evidences that μ increases linearly with the thickness of the active layer, independently on the film structure (single or multilayer). In contrast, the exhaustion time increases linearly with the thickness of the active layer only in the case of the three-layer structures; instead the exhaustion time of the SL-aPET film, whose active phase is directly exposed to the air, is the lowest among all.

All these observations demonstrate that the incorporation of the active layer in a multilayer structure does not alter its reactivity toward the oxygen and that controlling the thickness of the

SL-PET	TL3	SL-aPET
		
$\Delta E_{CMC(1:1)}{}^{\#} = 7.8 \pm 1.2$	$\Delta E_{CMC(1:1)}{}^{\#} = 2.1 \pm 0.1$	$\Delta E_{CMC(1:1)}{}^{\#} = 5.7 \pm 0.6$

$^{\#}\Delta E_{CMC(1:1)} \approx 1$ corresponds to a just noticeable difference

Figure 7. Pictures of apple slices packaged in the single layer neat (SL-PET) and active (SL-aPET) PET films and in the three layer (TL3) active one, taken after 15 days of storage at 8°C, together with the corresponding values of the color difference $\Delta E_{CMC(1:1)}$. [Color figure can be viewed in the online issue, which is available at wileyonlinelibrary.com.]

Table VI. Total Acidity and Sugars Content of Fresh-Cut Apple Slices, Before Storage and After 15 Days of Storage at 8°C in Three Different Package Systems

			Sugars (g/100 g)			
	Packaging type	Total acidity (%)	Fructose	Glucose	Saccarose	Total
Before storage	As fresh-cut	0.15 ± 0.02	5.0 ± 0.3	2.5 ± 0.3	2.5 ± 0.3	10.0 ± 0.3
After 20 days of storage at 8°C	SL-PET	0.55 ± 0.03	7.3 ± 0.6	2.3 ± 0.5	2.9 ± 0.4	12.6 ± 0.5
	TL3	0.12 ± 0.02	5.7 ± 0.2	2.8 ± 0.2	3.0 ± 0.2	11.6 ± 0.2
	SL-aPET film	0.35 ± 0.03	6.9 ± 0.4	2.6 ± 0.3	2.9 ± 0.4	12.4 ± 0.4

external PET layers can be a useful strategy to regulate the oxygen scavenging performance in such multilayer active structure.

After the oxygen scavenging activity exhaustion, all active films were submitted to oxygen permeability measurements, in order to evaluate their steady-state oxygen transport properties. The same measurements were performed on the SL-PET film, too, for comparison. The obtained results are reported in Table IV.

It can be observed that the presence of the active phase in the film formulation give a small reduction in the permeability and O_2TR values of the exhaust samples. The amount of these changes depends on the relative layer thickness and increases with the active phase in the system.

Correspondingly, compared with the SL-PET film, a change in both diffusivity and solubility coefficients, can be also noticed for all the active systems. Two factor can contribute to these results: (i) the chemical modifications occurred in the active systems because of the oxygen scavenging by AMS, and (ii) the changes in the PET crystalline morphology due to both the presence of the active phase and the thermomechanical environment applied during the coextrusion process, as it comes out from DSC measurements, which results are reported in Table V.[38]

The DSC data show only minor differences in the crystallinity degree and in the thermal parameters of the analyzed films. However, on this point it has to emphasized that DSC data can only give indicative information about the initial crystalline morphology of the samples, as they combine the response of the PET fraction that has crystallized on processing and those that have crystallized during the DSC heating run. Nevertheless, as it can be seen from the thermograms of the SL-PET, SL-aPET, and TL3 films, compared in Figure 6, the different initial morphological state of the samples can be mainly evidenced in the cold crystallization peak temperature (T_{cc}), which increases in the order SL-aPET < SL-PET ≈ TL3. The change is a consequence of the slowdown of the crystallization kinetics that can be related to the lower molecular mobility (i.e., higher viscosity) of the neat PET compared with the active system.[33] Moreover, there is also a progressive increase in the half-height width ($W_{0.5}$) of the cold crystallization peak in the order SL-aPET ($W_{0.5} = 4.2°C$) < SL-PET ($W_{0.5} = 6.8°C$) < TL3 ($W_{0.5} = 10.3°C$), which suggests a more inhomogeneous crystal morphology.

However, the data of Table IV show also that the O_2 permeability values of all the three-layer exhaust samples fit well the permeability coefficients calculated according to the classical theory of steady-state permeation through conventional (not active) polymeric films, which applies a series model to predict the permeability coefficient of a multilayer film (P_T) from that of its individual component layer, as follows:

$$P_T = \frac{L_T}{\sum_i \frac{L_i}{P_i}} \quad (15)$$

where L_T is total thickness, L_i is thickness of individual layer, and P_i is permeability of individual layer.[5] The accordance between the experimental and calculated P_T values suggests that the structure and properties of each layer in the three-layer films are identical with those of corresponding single layer and that the interphase (created along the interface due to interdiffusion of the layer components) does not perceptibly affect the three-layer film properties.

With the aim to investigate the efficacy of the active three layer structures realized in this work in preserving fresh foods by oxidation, preliminary shelf life tests on fresh-cut apple slices were carried out, using Golden Delicious apple cultivar as model of oxygen-sensitive fresh food. Two untreated fresh-cut apple slices (~40 g) were packaged both in the three-layer TL3 active film and in the single layer active SL-aPET and SL-PET films, and then stored at 8°C.

In order to evaluate both the changes in the quality and the degradation level of the fresh-cut apple slices during their storage, all packaged samples were analyzed after 15 days of refrigerated storage to measure their variation in color, acidity, and sugar content.[48] The color difference ΔE was selected as the most suitable parameter to measure cut surface browning, whereas the total acidity and the sugar content were chosen as quality indicators of the nutritional values of the fruits.[49,50]

The pictures of the packaged samples, taken after 15 days of storage at 8°C, together with the values of the color difference ΔE, are reported in Figure 7. The Figure shows that the chromatic change ΔE is not noticeable only for the apple slices packaged in the TL3 film. Instead in the case of the apple slices packaged in both the single layer films the ΔE values are high enough to be perceived by the human eye; the effect is particularly marked in the case of the SL-PET film. These observations demonstrate that the TL3 film is effective in slowing the oxidative phenomena of the apple cut surfaces reducing their browning. The result is to be related to TL3 film ability to lower the O_2 atmosphere in the package, as it came out from the oxygen scavenging experiments.

The values of the acidity and sugar content are reported in Table VI. Again, comparing the total acidity of the samples, it comes out that only the TL3 film preserve the apple slices from change in their acidity level, which is directly related to the sweet taste of the fruit, whereas the SL-PET film shows the worst performance. However, all samples maintain essentially the original sugar content whatever the type of film used for the packaging; the measured interchange between various sugars is probably own to metabolic activity in the fruit.[50]

All the results of the preliminary shelf life tests suggest that, among the packaging solutions experimented in this work, the TL3 film is the most efficient in preserving the quality of oxygen-sensitive foods.

CONCLUSIONS

In this work, three layer active polyester films have been realized by coextrusion process and characterized in terms of both oxygen scavenging performance and oxygen permeability, measured after the film activity exhaustion. O_2 absorption measurements in continuous mode have shown that all the three layer analyzed films show a longer exhaustion time than those of the monolayer active films and have pointed out the role of relative layer thickness of the multilayer structures in controlling the scavenging capacity, the activity time and the oxygen absorption rate. In particular, both the scavenging capacity and the activity time increase linearly with the thickness of the active internal layer of the three layer structures, whereas the kinetic of the oxygen absorption reaction at short times decreases proportionally with the thickness of the external neat PET layer. Moreover, steady state oxygen transport tests conducted on the exhaust films have shown that the presence of the active phase in the multilayer films slightly modifies the steady transport properties in comparison to the neat PET, giving a small reduction in the permeability and O_2TR values. The effect may be related to the different morphological state developed upon processing for the films containing different amounts of active phase (i.e. with different relative layer thickness). Finally, as demonstrated by packaging tests on fresh cut untreated apples, the active three layer PET films, produced and analyzed in this work, show potential for application in active packaging technology.

ACKNOWLEDGMENTS

This research was partially supported by National Operation Project Program (PON-SafeMeat-Italy 01_01409).

The authors gratefully acknowledge prof. Giuseppe Mensitieri from the Department of Chemical, Materials and Industrial Production Engineering, University of Naples "Federico II" (Italy), for the helpful discussions and valuable comments, and Dr. Francesco Marra and Tesfaye Faye Bedane from the Department of Industrial Engineering, University of Salerno (Italy), for model calculations.

REFERENCES

1. Labuza, T. P.; Breene, W. M. *J. Food Process. Pres.* **1989**, *13*, 1.
2. Kelly, R. S. A. *J. Plast. Film Sheet.* **1987**, *3*, 41.
3. Lange, J.; Wyser, Y. *Packag. Technol. Sci.* **2003**, *16*, 149.
4. Mueller, K.; Schoenweitz, C.; Langowski, H. C. *Packag. Technol. Sci.* **2012**, *25*, 137.
5. Robertson, G. L., Ed. Food Packaging: Principles and Practice, 2nd ed.; CRC Press: Boca Raton, **2013**; Chapters 4–5.
6. Vermeiren, L.; Heirligs, L.; Devlieghere, F.; Debevere, J. In Novel Food Packaging Techniques; Ahvenainen R., Ed.; Woodhead Publishing Limited: Cambridge UK, **2003**; Chapter 3.
7. Devlieghere, F.; Vermeiren, L.; Debevere, J. *Int. Dairy J.* **2004**, *14*, 273.
8. Arvanitoyannis, I. S.; Oikonomou, G. In Modified Atmosphere and Active Packaging Technologies; Arvanitoyannis, I., Ed.; CRC Press: Boca Raton, **2012**; Chapter 14.
9. Brody, A. L.; Strupinsky, E.; Kline, L. R.Active Packaging for Food Applications. CRC Press: Boca Raton, **2001**
10. Gómez-Estaca, J.; López-de-Dicastillo, C.; Hernández-Muñoz, P.; Catalá, R.; Gavara, R. *Trends Food Sci. Technol.* **2014**, *35*, 42.
11. Jamshidian, M.; Tehrany, E. A.; Imran, M.; Akhtar, M. J.; Cleymand, F.; Desobry, S. *J. Food Eng.* **2012**, *110*, 380.
12. Lopez-Rubio, A.; Almenar, E.; Hernandez-Muñoz, P.; Lagaròn, J. M.; Català, R.; Gavara, R. *Food Rev. Int.* **2004**, *20*, 357.
13. Nerín, C.; Tovar, L.; Salafranca, J. *J. Food Eng.* **2008**, *84*, 313.
14. Vermeiren, L.; Devlieghere, F.; Beest, M. V.; Kruijf, N. D.; Debevere, J. *Trends Food Sci. Technol.* **1999**, *10*, 77.
15. Matche, R. S.; Sreekumar, R. K.; Raj, B. *J. Appl. Polym. Sci.* **2011**, *122*, 55.
16. Yeh, J.-T.; Cui, L.; Chang, C.-J.; Jiang, T.; Chen, K.-N. *J. Appl. Polym. Sci.* **2008**, *110*, 1420.
17. Scafati, S.; Boragno, L.; Losio, S.; Conzatti, L.; Lanati, S.; Sacchi, M.; Stagnaro, P. *J. Appl. Polym. Sci.* **2014**, *131*; doi: 10.1002/app.39503.
18. Cardona, E. D.; del Pilar Noriega, M.; Sierra, J. D. *J. Plast. Film Sheet.* **2012**, *28*, 63.
19. Charles, F.; Sanchez, J.; Gontard, N. *J. Food Eng.* **2006**, *72*, 1.
20. Gibis, D.; Rieblinger, K. *Procedia Food Sci.* **2011**, *1*, 229.
21. Llorens, A.; Lloret, E.; Picouet, P. A.; Trbojevich, R.; Fernandez, A. *Trends Food Sci. Technol.* **2012**, *24*, 19.
22. Souza Cruz, R.; Peruch Camilloto, G.; dos Santos Pires, A. C. Oxygen Scavengers: An Approach on Food Preservation, Structure and Function of Food Engineering; Eissa, A. A, Ed., **2012**; InTech, ISBN: 978-953-51-0695-1; DOI: 10.5772/48453. Available from: http://www.intechopen.com/books/structure-and-function-of-food-engineering/oxygen-scavengers-an-approach-on-food-preservation (Last accessed April 7, 2014).
23. Trindade, M. A.; Montes Villanueva, N. D.; Vendemiatto Antunes, C.; de Alvarenga Freire, M. T. *Brazil. J. Food Technol.* **2013**, *16*, 216.
24. Anthierens, T.; Ragaert, P.; Verbrugghe, S.; Ouchchen, A.; De Geest, B. G.; Noseda, B.; Mertens, J.; Beladjal, L.; De Cuyper, D.; Dierickx, W.; Du Prez, F.; Devlieghere, F. *Innov. Food Sci. Emerg. Technol.* **2011**, *12*, 594.
25. Bheda, J. H.; Moore, I. V. (BM. Invista North America S.a.r.L.). U. S. Patent 7,294,671 **2007**.

26. Blinka, T. A.; Edwards, F. B.; Miranda, N. R.; Speer, D. V.; Thomas, J. A. W. R. Grace and Co.-Conn. U. S. Patent 5,834,079 **1998**.
27. Cahill, P. J.; Chen, S. Y. BP Amoco Corporation. U. S. Patent 6,083,585 **2000**.
28. Dainelli, D.; Gontard, N.; Spyropoulos, D.; Zondervan-van den Beuken, E.; Tobback, P. *Trends Food Sci. Technol.* **2008**, *19*, S103.
29. Miltz, J.; Perry, M. *Packag. Technol. Sci.* **2005**, *18*, 21.
30. Sängerlaub, S.; Gibis, D.; Kirchhoff, E.; Tittjung, M.; Schmid Kajetan Müller, M. *Packag. Technol. Sci.* **2013**, *26*, 17.
31. Share, P. E.; Pillage, K. R. Valspar Sourcing, Inc. U. S. Patent 7,244,484 **2007**.
32. Tung, D.; Sisson, E.; Leckonby, R. A. M & G USA Corporation. U. S. Patent 6,780,916 **2004**.
33. Tibbitt, J. M.; Cahill, P. J.; Rotter, G. E.; Sinclair, D. P.; Brooks, G. T.; Behrends, T. R. BP Corporation North America Inc. U. S. Patent 7,214,415 **2007**.
34. Di Maio, L.; Scarfato, P.; Avallone, E.; Galdi, M. R.; Incarnato, L. *AIP Conf. Proc.* **2014**, *1593*, 338.
35. Mahajan, K.; Lofgren, E. A.; Jabarin, S. A. *J. Appl. Polym. Sci.* **2013**, *129*, 2196.
36. Mahajan, K.; Lofgren, E. A.; Jabarin, S. A. *J. Appl. Polym. Sci.* **2013**, *130*, 4273.
37. Galdi, M. R.; Nicolais, V.; Di Maio, L.; Incarnato, L. *Packag. Technol. Sci.* **2008**, *21*, 257.
38. Galdi, M. R.; Incarnato, L. *Packag. Technol. Sci.* **2011**, *24*, 89.
39. Iroh, J. O. Polymer Data Handbook; Oxford University Press: New York, **1999**.
40. Clarke, F. J. J.; McDonald, R.; Rigg, B. *J. Soc. Dyers Colour.* **1984**, *100*, 117.
41. Kim, A.; Kim, H.; Park, S. *J. Opt. Soc. Korea* **2011**, *15*, 310.
42. Gillen, K. T.; Clough, R. L. *Polymer* **1992**, *33*, 4358.
43. Carranza, S.; Paul, D. R.; Bonnecaze, R. T. *J. Membr. Sci.* **2010**, *360*, 1.
44. Ferrari, M. C.; Carranza, S.; Bonnecaze, R. T.; Tung, K. K.; Freeman, B. D.; Paul, D. R. *J. Membr. Sci.* **2009**, *329*, 183.
45. Solovyov, S. E.; Goldman, A. Y. *J. Appl. Polym. Sci.* **2006**, *100*, 1966.
46. Carranza, S.; Paul, D. R.; Bonnecaze, R. T. *J. Membr. Sci* **2012**, *399-400*, 73.
47. Crank, J. The Mathematics of Diffusion; Clarendon Press: Oxford, **1975**; p 51.
48. Rico, D.; Martín-Diana, A. B.; Barat, J. M.; Barry-Ryan, C. *Trends Food Sci. Technol.* **2007**, *18*, 373.
49. Gil, M. I.; Gorny, J. R.; Kader., A. A. *HortScience* **1988**, *33*, 305.
50. Veberic, R.; Schmitzer, V.; Petkovsek, M. M.; Stampar, F. *J. Food Sci.* **2010**, *75*, S461.